Research Journal of Applied Sciences, Engineering and Technology 11(9): 934-949, 2015
DOI: 10.19026/rjaset.11.2133
ISSN: 2040-7459; e-ISSN: 2040-7467

Submitted: March 14, 2015 Accepted: June 18, 2015 Published: November 25, 2015

Research Article

A New Estimation Model to Control DVR for Mitigating Voltage Sags in Distribution Systems

[1]P. Sasi Kiran and [2]T. Gowri Manohar
[1]Department of Electrical and Electronics Engineering, K.L. University,
Vaddeswaram, Guntur, Andhra Pradesh, India
[2]Department of Electrical and Electronics Engineering, College of Engineering, S.V. University,
Tirupathi, A.P., India

Abstract: In this study proposed, for voltage sag mitigation an estimation method based on Extended Kalman Filter (EKF) is suggested. The suggested EKF based estimation technique is applied to help the control algorithm for producing reference signals of Voltage Source Converter (VSC) of DVR. DVR offers the compensation voltage as output which is inserted in the connected line. With this estimation method, voltage sag issues are found out with precision and faster performance to revoke out the sag appearance in sensitivity load connected distribution systems. The presentation of the suggested estimation technique is examined in terms of presenting the fundamental sinusoidal waveform to the nonlinear sensitive load. The confirmation of the suggested estimation algorithm is carried out on MATLAB working platform. Simulation effects are inspected and suggested one is compared with Linear Kalman Filter (LKF).

Keywords: Control algorithm, DVR, EKF, estimation technique, LKF, voltage sag

INTRODUCTION

There is an ever increasing practice of sophisticated sensitive electronic equipments (Marefatjou and Sarvi, 2012) in the distribution system. It is Distribution System Operator's (DSO) duty to guard these sensitive loads from any type of Power Quality (PQ) disturbances (Ipinnimo *et al*., 2013; Ghosh *et al*., 2012). For the customer, the harms can be very costly, ranging from minor quality differences to production downtime and equipment failure which become economic loss for utilities too (Singh *et al*., 2013; Raman and Singh, 2014). In distribution system voltage sags or dips are the grown distress of PQ problems. These are caused by rapid increases in loads such as motors starting or electric heaters turning on or quick increases in source impedance or slack connection or short circuits or faults (Gupta *et al*., 2010; Hussain and Praveen, 2012). Voltage sag is termed as voltage amplitude ranging from 0.1 to 0.9 p.u with a duration lasting for half a cycle to 1 min (Tanti *et al*., 2012; Vetrivel *et al*., 2013) according to IEEE standards. For accomplishing a dependable and high quality voltage, CPD: DVR is the recently developed idea based on the application of power electronic controllers to alleviate the voltage sags (Hannan and Mohamed, 2012; Pakharia and Gupta, 2012; Tiwari and Gupta, 2010a). Commonly, a DVR contains five components: an energy storage system or an alternative power source, a VSC which changes the DC voltage from the energy storage system to the necessary AC voltage to nullify disturbances, greatly sags only, a coupling transformer which is series coupled in the feeder, an output filter to revoke the harmonics brought in by the PWM process of the VSC and a control strategy for VSC (Torres *et al*., 2013; Deepa and Rajapandian, 2010). On the other hand, the performance of the DVR greatly relies on their control strategies which keep constant voltage magnitude by finding out the reference voltages for VSC (Dib *et al*., 2011). Nevertheless, this is only found out according to the degree of disturbances in supply voltages (Tiwari and Gupta, 2010b). As a result, with the suitable control strategy, it inserts three single phase AC output voltages in series with the distribution feeder to continue the wanted amplitude and waveform for load voltage even when the system voltage is unbalance or distorted (Babaei *et al*., 2010).

Generally, DVR is installed on a critical load feeder where it functions in two modes in distribution systems: low loss standby mode when no sag condition happened and provides voltage for compensation of sag when it is in transient state mode (Kavitha *et al*., 2013). In transient mode, it is in addition feasible to compensate voltage sag by three separate methods: pre-sag, in-phase and minimal energy compensation

Corresponding Author: P. Sasi Kiran, Department of Electrical and Electronics Engineering, K.L. University, Vaddeswaram, Guntur, Andhra Pradesh, India

methods (Kandil *et al*., 2013). In pre-sag: it inserts the difference voltage among during-sag and pre-sag voltages to the system. In in-sag: it inserts voltage in phase with supply voltage to compensate the voltage magnitude only where loads can endure phase angle jumps and in minimal energy compensation method; it provides the active power to as per the DSO's requirement (El-Gammal *et al*., 2011). Voltage sag mitigation by DVR is carried out by means of different control techniques based on the three compensation methods. In each of the control methods, detection of voltage sag occurrence and estimation of reference voltages for VSC in advance performs a main role for voltage sag mitigation by DVR.

RECENT LITERATURE REVIEW: A RESEARCH BRIEF

Using DVR, there are many research works offered on voltage sag mitigation in literature. A few of them are assessed here. A control scheme for the DVR has been suggested by Ajaei *et al*. (2011) to attain quick response and successful sag compensation capabilities. The suggested method controlled the magnitude and phase angle of the injected voltage for each phase individually. To estimate the magnitude and phase of the measured voltages fast least error squares digital filters were applied. The employed least error squares estimated filters very much decrease the effects of noise, harmonics and disturbances on the estimated phasor parameters. This facilitated the DVR to identify and compensate voltage sags precisely, under linear and nonlinear load conditions. The suggested control system did not require any phase-locked loops. It moreover successfully restricted the magnitudes of the modulating signals to prevent over modulation. In addition, individually controlling the injected voltage in each phase facilitated the DVR to adjust the negative- and zero-sequence components of the load voltage and the positive-sequence component.

Using DVR an auxiliary control approach for downstream fault current interruption has been suggested by Ajaei *et al*. (2013) in a radial distribution line. The suggested controller increased the voltage-sag compensation control of the DVR. It did not need phase-locked loop and separately controlled the magnitude and phase angle of the injected voltage for each phase. Fast least error squares digital filters were applied to calculate approximately the magnitude and phase of the measured voltages and successfully decreased the impacts of noise, harmonics and disturbances on the estimated phasor parameters and this facilitated efficient fault current interrupting even under arcing error conditions.

An easy generalized algorithm has been proposed by Kanjiya *et al*. (2013) and Abdollahzadeh *et al*. (2014) based on basic Synchronous Reference Frame (SRF) theory for the generation of instant reference compensating voltages for controlling a DVR. It applied the fundamental positive-sequence phase voltages extorted by sensing only two unbalanced and/or distorted line voltages. The algorithm was broad enough to handle linear and nonlinear loads. With a distribution feeder the compensating voltages when inserted in series by three single-phase H-bridge VSCs with a constant switching frequency hysteresis band voltage controller tightly adjusted the voltage at the load terminals against PQ problems on the source side.

A novel fast-converged estimation approach has been suggested by Abdollahzadeh *et al*. (2014). Which directly extorts amplitudes and phase angles of symmetrical components of needed frequencies from harmonic-distorted network voltages. The sufficient convergence time and precision of this approach made it relevant in DVR as an application in which the rapidity of response was of the most significant obligations. According to this intention, sensitivity analyses were organized to evaluate the impacts of sag depth variations, phase angle jumps and frequency variations on the performance of the suggested algorithm.

Different voltage injections schemes for DVR has been suggested by Jayaprakash *et al*. (2014). Were examined with particular focus employed to minimize the rating of the VSC applied in DVR. A novel control technique was suggested to control the capacitor-supported DVR. With a reduced-rating VSC the control of a DVR was shown. The reference load voltage was estimated by means of the unit vectors. The SRF theory was applied for the change of voltages from rotating vectors to the stationary frame. Using a reduced-rating DVR the compensation of the voltage sag, swell and harmonics was expressed.

There is numerous control algorithms such as fuzzy logic, deadbeat control and vector control have been employed for DVR. To compensate the voltage sag is the intention of these control algorithms. In the stated control algorithms; fuzzy logic requires the precise determination fuzzy membership functions and fuzzy rule formulations which are probable by expert's knowledge only. Deadbeat control algorithm requires to be adjusted regularly for its control gains and vector control is a difficult technique in planning. For finding out the reference voltages these disadvantages are making the DVR's control algorithm more indecisive. To develop the presentation of the control strategy, it requires a good recognition technique for any type of voltage sag disturbance. It should precisely estimate the symmetrical components of the deformed distribution system voltages. It is feasible to produce the reference voltages in lesser time with the good estimation technique only and faster control action is carried out. If the estimation is poor, it is unfeasible to produce the precise reference voltages for VSC which makes the DVR's compensation deplorable. It illustrates that numerous techniques such as least error square digital filter, SRF theory, etc., have been brought in the

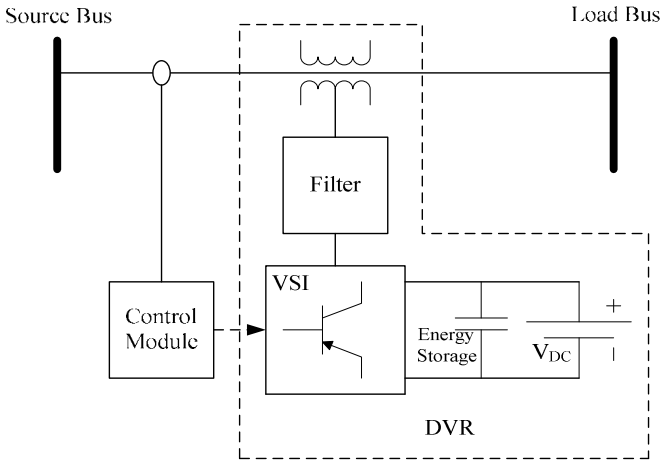

Fig. 1: Single line diagram of the DVR

process of finding out the reference voltages from the connected work. In the stated techniques; they require to minimize the least error squares to zero which is not all the time possible and SRF theory employs the d-q transformations which can never work with deformed network voltages. These matters in estimating the compensating reference voltages make them indecisive to execute voltage sag mitigation. As a result, it requires good estimation technique for finding out the voltage sag occurrence in the system for improved compensation. In literature, a very little works are offered regarding estimating techniques prior to the control algorithm design for voltage sag compensation. Hence, the above stated disadvantages have inspired me to do this research work.

METHODOLOGY

EKF model aided control module for DVR: The faults in distribution system may be due to the short circuits or unintentional contacts of line to ground, double line to ground, triple line, etc. The period of these faults are sometimes less than a power cycle or even more than a second. This situation upsets the amplitude or phase or both of the system supply voltages. Hence, a voltage sag or swell scenario comes out. The control algorithm of the DVR is proposed for mitigating those voltage sags in this section. The suggested control algorithm relies on the symmetrical components of the supply voltages. By the suggested control algorithm the voltage sag distortion is predetermined and compensates it before feeding to the load. Thus, any sensitive load linked to it is securely guarded. The suggested control algorithm contains estimation model and control modules which are elucidated in next subsections. Before that, single line diagram of suggested DVR system is made clear. It is illustrated in Fig. 1 as follows.

The single line diagram of suggested DVR system is shown in Fig. 1. From Fig. 1, it says that, the DVR is joined between source bus and load bus. Load bus voltage is sheltered with the assist of suggested control algorithm and holds back it to the fundamental frequency of supply voltage without distortion in amplitude and phase angles. By injecting compensating voltage by means of the series transformer of DVR this action is executed. A sag detection model and concerned controller model are needed in order to compensate voltage sag precisely. In this document, the sag detection model contains EKF model which estimates instant symmetrical components of supply voltages and is compared with reference values to make sure the sag appearance. Suitable control action is executed after the detection of sag, by control module. The block diagram of the suggested control approach is illustrated in Fig. 2.

The block diagram of the suggested control scheme based on EKF model is offered in Fig. 2. From the block diagram of the suggested control algorithm, it says that, EKF model estimates the symmetrical components of the supply voltages and are compared with reference symmetrical components to offer the injecting voltage by the DVR such that the detected sag is reimbursed. The reference symmetrical components are the pre-sag symmetrical components which are found out by the suggested control scheme as detailed in subsequent subsection.

EKF model for estimating symmetrical components: The determination of symmetrical components is executed in this subsection. To find out them, initially, it is essential to symbolize the suggested system in state equations. The state equations are obtained from the measured voltages representations in terms of their symmetrical components. With those state equations, state variables are chosen and suitable state vector and measurement vector equations are obtained. EKF model estimates the symmetrical components from these state equations.

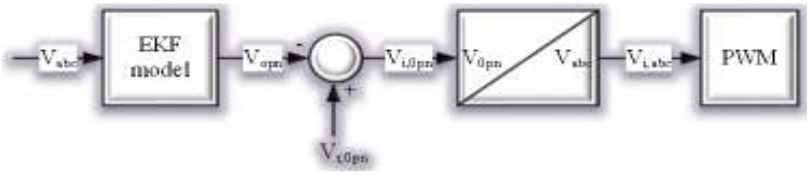

Fig. 2: Block diagram of the proposed control structure

Developing state equations from measurements: The measured supply voltages of proposed system can be written as:

$$\left.\begin{aligned} V_a(t) &= V_{am}\sin(\omega t+\phi_a)\\ V_b(t) &= V_{bm}\sin(\omega t+\phi_b)\\ V_c(t) &= V_{cm}\sin(\omega t+\phi_c)\end{aligned}\right\} \tag{1}$$

where, $V_a(t)$, $V_b(t)$ and $V_c(t)$ are measured three phase supply voltages respectively at time instant t. V_{am} and ϕ_a, V_{bm} and ϕ_b and V_{cm} and ϕ_c are the amplitude and phase of the measured three phase supply voltages respectively. ω is the system frequency. Using Eq. (1), the detailed symmetrical components of the supply voltages are given as:

$$\left.\begin{aligned} V_a(t) &= \overrightarrow{V_0}+\overrightarrow{V_p}+\overrightarrow{V_n} = V_{0m}\sin(\omega t+\phi_0)+V_{pm}\sin(\omega t+\phi_p)+V_{nm}\sin(\omega t+\phi_n)\\ V_b(t) &= \overrightarrow{V_0}+a^2.\overrightarrow{V_p}+a.\overrightarrow{V_n} = V_{0m}\sin(\omega t+\phi_0)+V_{pm}\sin(\omega t+\phi_p-120)+V_{nm}\sin(\omega t+\phi_n+120)\\ V_c(t) &= \overrightarrow{V_0}+a.\overrightarrow{V_p}+a^2.\overrightarrow{V_n} = V_{0m}\sin(\omega t+\phi_0)+V_{pm}\sin(\omega t+\phi_p+120)+V_{nm}\sin(\omega t+\phi_n-120)\end{aligned}\right\} \tag{2}$$

where, $a = 1\angle 120°$ and $a^2 = 1\angle 240°$. $\vec{V}_0$, $\vec{V}_p$ and $\vec{V}_n$ are the zero, positive and negative sequence component vectors of measured supply voltages respectively. V_{0m} and ϕ_0, V_{pm} and ϕ_p and V_{nm} and ϕ_n are the amplitude and phase of zero, positive and negative sequence components respectively. In Eq. (2), we have some sine and cosine functions such as $\sin(\omega t + \phi_p + 120)$, $\sin(\omega t + \phi_n + 120)$, etc. Therefore, Eq. (2) can be further decomposed as:

$$\left.\begin{aligned} V_a(t) &= V_{0m}\left[\sin(\omega t).\cos(\phi_0)+\cos(\omega t).\sin(\phi_0)\right]+V_{pm}\left[\sin(\omega t).\cos(\phi_p)+\cos(\omega t).\sin(\phi_p)\right]\\ &\quad +V_{nm}\left[\sin(\omega t).\cos(\phi_n)+\cos(\omega t).\sin(\phi_n)\right]\\ V_b(t) &= V_{0m}\left[\sin(\omega t).\cos(\phi_0)+\cos(\omega t).\sin(\phi_0)\right]\\ &\quad +V_{pm}\begin{bmatrix}\sin(\omega t).\cos(\phi_p).\cos(-120)+\cos(\omega t).\sin(\phi_p).\cos(-120)\\ +\cos(\omega t).\cos(\phi_p).\sin(-120)-\sin(\omega t).\sin(\phi_p).\sin(-120)\end{bmatrix}\\ &\quad +V_{nm}\begin{bmatrix}\sin(\omega t).\cos(\phi_n).\cos(120)+\cos(\omega t).\sin(\phi_n).\cos(120)\\ +\cos(\omega t).\cos(\phi_n).\sin(120)-\sin(\omega t).\sin(\phi_n).\sin(120)\end{bmatrix}\\ V_c(t) &= V_{0m}\left[\sin(\omega t).\cos(\phi_0)+\cos(\omega t).\sin(\phi_0)\right]\\ &\quad +V_{pm}\begin{bmatrix}\sin(\omega t).\cos(\phi_p).\cos(120)+\cos(\omega t).\sin(\phi_p).\cos(120)\\ +\cos(\omega t).\cos(\phi_p).\sin(120)-\sin(\omega t).\sin(\phi_p).\sin(120)\end{bmatrix}\\ &\quad +V_{nm}\begin{bmatrix}\sin(\omega t).\cos(\phi_n).\cos(-120)+\cos(\omega t).\sin(\phi_n).\cos(-120)\\ +\cos(\omega t).\cos(\phi_n).\sin(-120)-\sin(\omega t).\sin(\phi_n).\sin(-120)\end{bmatrix}\end{aligned}\right\} \tag{3}$$

The above equation can be simplified by representing in matrix form. It is given as follows:

$$\begin{bmatrix}V_a(t)\\ V_b(t)\\ V_c(t)\end{bmatrix} = \begin{bmatrix}h_{11} & h_{12} & h_{13} & h_{14} & h_{15} & h_{16}\\ h_{21} & h_{22} & h_{23} & h_{24} & h_{25} & h_{26}\\ h_{31} & h_{32} & h_{33} & h_{34} & h_{35} & h_{36}\end{bmatrix}\begin{bmatrix}V_{0m}.\cos(\phi_0)\\ V_{0m}.\sin(\phi_0)\\ V_{pm}.\cos(\phi_p)\\ V_{pm}.\sin(\phi_p)\\ V_{nm}.\cos(\phi_n)\\ V_{nm}.\cos(\phi_n)\end{bmatrix} \tag{4}$$

where, h_{ij} is i^{th}, j^{th} element of the measurement matrix from Eq. (3). If we select the symmetrical components based functions as state variables, the state vector variables can be given as:

$$X(t)=\begin{bmatrix}x_1(t)\\x_2(t)\\x_3(t)\\x_4(t)\\x_5(t)\\x_6(t)\end{bmatrix}=\begin{bmatrix}V_{0m}.\cos(\phi_0)\\V_{0m}.\sin(\phi_0)\\V_{pm}.\cos(\phi_p)\\V_{pm}.\sin(\phi_p)\\V_{nm}.\cos(\phi_n)\\V_{nm}.\cos(\phi_n)\end{bmatrix} \quad (5)$$

From Eq. (4) and (5), the measurement equation of the suggested DVR system can be specified in simplified form as:

$$Z(t)=H(t).X(t) \quad (6)$$

where, $Z(t)$ is the measured three phase supply voltages at time instant t. $H(t)$ is the measurement matrix. Now, let us represent the state variables $X(t)$, in terms of discrete. It is given as follows:

$$\begin{bmatrix}x_1(k)\\x_2(k)\\x_3(k)\\x_4(k)\\x_5(k)\\x_6(k)\end{bmatrix}=\begin{bmatrix}V_{0m}.\cos(\phi_0)\big|_k\\V_{0m}.\sin(\phi_0)\big|_k\\V_{pm}.\cos(\phi_p)\big|_k\\V_{pm}.\sin(\phi_p)\big|_k\\V_{nm}.\cos(\phi_n)\big|_k\\V_{nm}.\cos(\phi_n)\big|_k\end{bmatrix} \quad (7)$$

where, $x_i(k)$ is the k^{th} sample of i^{th} state variable. From Eq. (7), it declares that, state variables are the sine or cosine functions of sequence component's amplitude and its phase angles. With this sine and cosine functions in considering, we can presume that there is a minor change in amplitude and phase angle between successive samples. As a result, the subsequent simplification for the state vector is valid:

$$\left.\begin{aligned}x_1(k+1)&\approx x_1(k)\\x_2(k+1)&\approx x_2(k)\\x_3(k+1)&\approx x_3(k)\\x_4(k+1)&\approx x_4(k)\\x_5(k+1)&\approx x_5(k)\\x_6(k+1)&\approx x_6(k)\end{aligned}\right\} \quad (8)$$

Therefore, the updating equation of the state variables is given as:

$$X(k+1)=X(k) \quad (9)$$

where, X (k + 1) and X (k) are the future and present sample of the state vector respectively. Now, from Eq. (6) and (9), the proposed nonlinear system can be represented as state equations. Therefore, the discrete process and measurement equations of the proposed system is given as:

$$\left.\begin{aligned}X(k+1)&=f\left[X(k),k\right]+w(k)\\Z(k)&=h\left[X(k),k\right]+v(k)\end{aligned}\right\} \quad (10)$$

where, $f[X(k), k]$ and $h[X(k), k]$ are nonlinear vector functions, namely, state matrix and measurement matrix respectively. $v(k)$ is a white noise vector with zero mean and $R(k)$ is as its covariance matrix. $w(k)$ is a vector that describes the state vector response due to a white noise input and has zero mean with $Q(k)$ as its covariance matrix. In the study, Eq. (10) is processed by EKF model to estimate the state variables of the proposed system and then determine the symmetrical components.

EKF estimation of state variables: EKF is the advanced version of the LKF and frequently employed in nonlinear systems. In EKF model, the nonlinear equations are linearized and then LKF process is employed. Now, the similar procedure is used and state variables are estimated for the nonlinear system as revealed in Eq. (10) which is in discrete process and measurement equations. Two update equations are significant in EKF mode and they are time update and measurement update equations. Kalman gain is calculated utilizing these two equations only and priori- and posteriori estimate of the state vector is calculated till the last sample is completed. In Fig. 3, the flow chart of EKF model is revealed.

From Fig. 3, the flow chart of the EKF model illustrates the step by step process for estimating the state variables. Now, with the first considerations, the discrete-time EKF algorithm for the state estimation process contains two steps. It is as specified as follows:

Step 1: In this step, EKF model is initialized for estimation. Here, for initialization, average value of the state variable is computed. It is set as the posteriori estimate of the state vector. Then, using the average value, error value is computed for all variables. Based on these error values, their co-variance matrix is computed and set as posteriori estimate of error co-variance matrix for EKF model process. It is given as follows.

Initialization of the EKF model at k = 0:

$$\left.\begin{aligned}\hat{X}^{+}(0)&=E\left[X(0)\right]\\P^{+}(0)&=E\left[\left(X(0)-\hat{X}^{+}(0)\right)\left(X(0)-\hat{X}^{+}(0)\right)^{T}\right]\end{aligned}\right\} \quad (11)$$

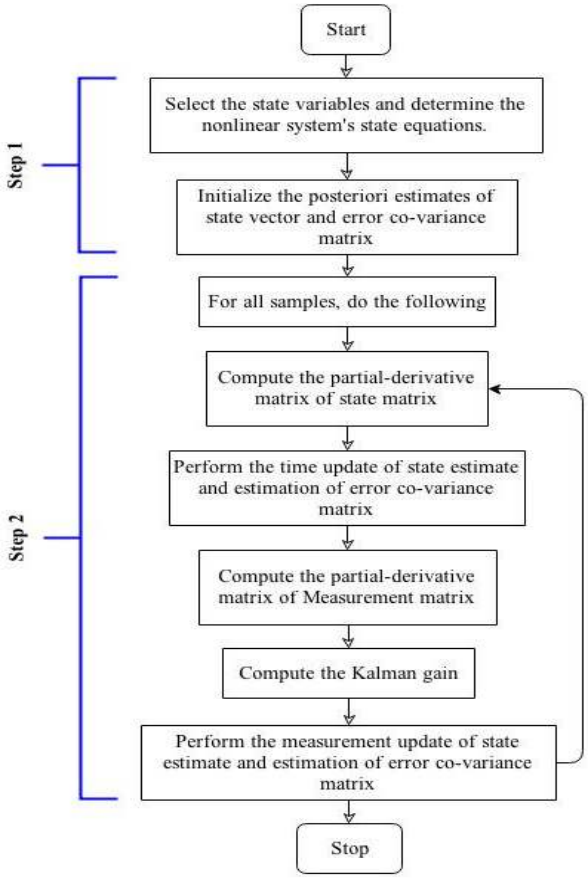

Fig. 3: The flow chart of EKF model

where, E indicates the average value, "^" indicates the estimate, "+" denotes the estimate is an a posteriori estimate. *P* is the co-variance matrix of error from average value.

Step 2: In this step, state variables are estimated by linearizing the nonlinear equations and applying LKF model process. It is repeated for all the sampled instants. It is given as follows.

For k = 1, 2, … Perform the following sub-steps:

- Compute the partial-derivative matrix of state matrix "f".

  In this sub-step, state matrix f is partial derivated and forwarded for next step. It is performed for linearizing the nonlinear equation. It is given as follows:

$$\Phi(k-1)=\frac{\partial f\left[\hat{X}^{+}(k-1),k-1\right]}{\partial X} \tag{12}$$

where, Φ (k - 1) is the linearized matrix of state matrix using posteriori estimate of state vector at (k - 1) instant.

- Perform the time update of state estimate and estimation of error co-variance matrix.

  In this sub-step, state equation and error co-variance matrix is estimated using previous measurement vector. It is as follows:

$$\left.\begin{aligned} P^{-}(k)&=\Phi(k-1)P^{+}(k-1)\Phi^{T}(k-1)+Q(k-1)\\ \hat{X}^{-}(k)&=f\left[\hat{X}^{+}(k-1),k-1\right]\end{aligned}\right\} \tag{13}$$

where, "-" superscript denotes the priori estimate.

- Compute the partial-derivative of measurement matrix "h".

  In this sub-step, measurement matrix "h" is partial derivated and forwarded for next step. It is performed for linearizing the nonlinear equation. It is given as follows:

$$H(k)=\frac{\partial h\left[\hat{X}^{-}(k),k\right]}{\partial X} \tag{14}$$

where, H (k) is the linearized matrix of measurement matrix using priori estimate of state vector at k instant.

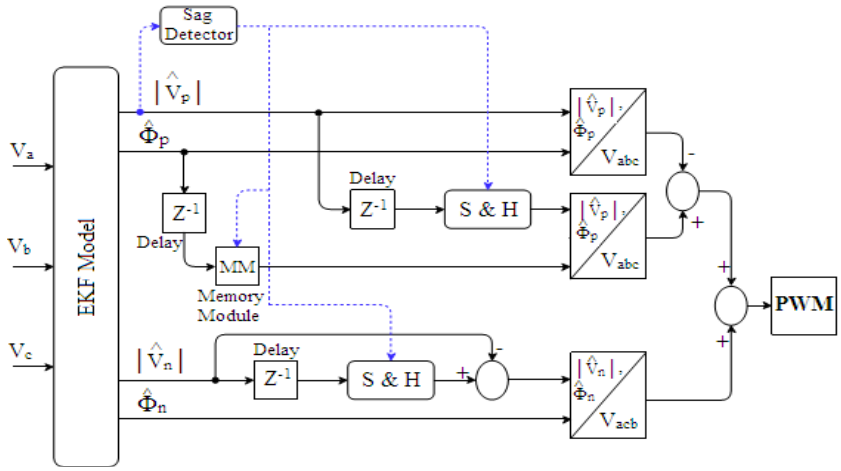

Fig. 4: The proposed control scheme aided by EKF model

- Calculate the filter coefficient at instant k, i.e., Kalman gain.
  In this sub-step, Kalman gain is computed for next sub-step purpose. It is given as follows:

$$K(k) = P^{-}(k)H^{T}(k)\left[H(k)P^{-}(k)H^{T}(k) + R(k)\right]^{-1} \quad (15)$$

  where, K (k) is the Kalman gain or filter co-efficient.
- Perform the measurement update of the state estimate and estimation of error covariance matrix.

In this sub-step, state equation and error co-variance matrix is estimated using present measurement vector. It is as follows:

$$\left.\begin{aligned} \hat{X}^{+}(k) &= \hat{X}^{-}(k) + K(k)\left(Z(k) - h\left[\hat{X}^{-}(k), k\right]\right) \\ P^{+}(k) &= \left(I - K(k)H(k)\right)P^{-}(k) \end{aligned}\right\} \quad (16)$$

where, I is the unit matrix. These are the five sub-steps in second step. Repeat these 5 steps for all the sampled measurement vector.

This is process by EKF model for estimating the state variables. From the state variables, symmetrical components are determined. It is given as follows:

$$\left.\begin{aligned} V_{0m} &= \sqrt{x_1^2 + x_2^2};\phi_0 = \tan^{-1}\left(\frac{x_2}{x_1}\right) \\ V_{pm} &= \sqrt{x_3^2 + x_4^2};\phi_p = \tan^{-1}\left(\frac{x_4}{x_3}\right) \\ V_{nm} &= \sqrt{x_5^2 + x_6^2};\phi_n = \tan^{-1}\left(\frac{x_6}{x_5}\right) \end{aligned}\right\} \quad (17)$$

From the Eq. (17), symmetrical components are determined and utilized by proposed control module will generate the proper control signals to the PWM of VSI. Now, the proposed control scheme after the estimation of symmetrical components is detailed in following subsection.

Proposed control strategy for generating injecting voltage: The control algorithm based on EKF model for the suggested DVR system is offered in this subsection. In the suggested control scheme, EKF model estimates three symmetrical components. The suggested control algorithm is proposed based on the positive and negative sequence components. It is revealed in Fig. 4.

From Fig. 4, it states that, system supply voltages are measured and fed to EKF model. This EKF model examines supply voltages and estimates the symmetrical components. After that for recognizing the sag occurrence the amplitude of the positive sequence component is examined. The sag appearance is recognized by checking the difference between estimated positive sequence and its nominal value. If the difference goes beyond the preset threshold value, it points out the sag detection. Sample and hold blocks are stimulated with the detection of sag appearance to recover the pre-sag voltages from memory module to offer reference signals. The purpose of compensation voltage for sags is specified as follows:

$$\left.\begin{aligned} V_p^{comp} &= V_p^{presag} - V_p^{sag} \\ &= \left|V_p^{presag}\right|\sin\left(\omega t + \phi_p^{presag}\right) - \left|V_p^{sag}\right|\sin\left(\omega t + \phi_p^{sag}\right) \end{aligned}\right\} \quad (18)$$

where, V_p^{presag} and V_p^{sag} are the pre-sag and sag voltages of positive sequence component correspondingly. $|V_p^{presag}|$ and ϕ_p^{presag} are the reference pre-sag amplitude and phase of positive sequence component from memory module. $|V_p^{sag}|$ and ϕ_p^{sag} are the real amplitude and phase of the positive sequence component during sag. Now, compensation is

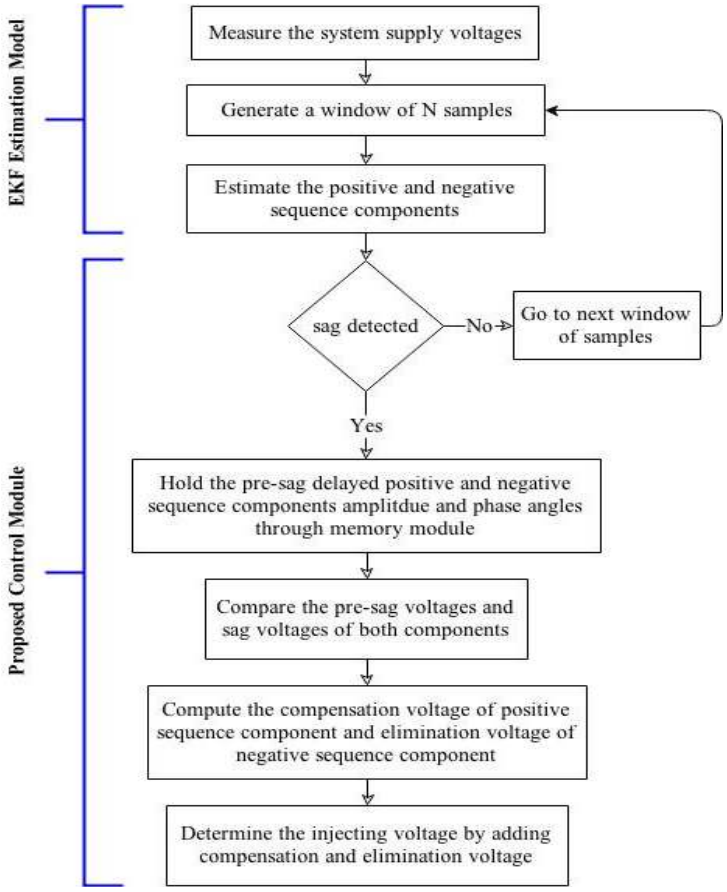

Fig. 5: The flow chart of the proposed control structure

executed with pre-sag voltages i.e., the compensation makes the system voltages go back to the pre-sag condition where sag is not there. The purpose of pre-sag voltage and computing eliminating voltage for negative sequence component is as well similar as positive sequence component. Both are added to offer the injecting voltage once the compensation and elimination voltages are calculated. This injecting voltage will reimburse the voltage sag happened at load bus. At present, the flow chart of the suggested control algorithm is illustrated as follows Fig. 5.

RESULTS AND DISCUSSION

The validation of the suggested EKF model based control module for suggested DVR system is offered in this section. For this purpose, the suggested method is checked on a three bus system where three phase power source is linked at one end and non-linear load connected other. DVR is linked on the power line joining another bus and load connected bus in this system. It is joined in series by three single phase transformers. They are coupled to VSC of DVR for inserting compensation voltage. In this proposed system, to make sure the compensation performance of the suggested method, a three phase fault is brought into the system. Because of this fault introduction in the system, it draws excess current from the lines and bus voltage will undergo voltage sag. This voltage sag is balanced by the suggested methodology and offers fundamental sinusoidal supply voltage to the nonlinear load without sag. Before going to the analysis on proposed controller, SIMULINK model of the proposed system is explained. It is given as follows.

In Fig. 6, the SIMULINK model of the suggested system based on DVR is offered. It contains three buses namely, B1, B2 and B3. The power source is joined at first bus and nonlinear source is joined at the third. In this system, DVR is joined between buses B2 and B3. In addition, the suggested test system contains 3 phase source block, R-L nonliner load block, fault generation block, DVR and its controller blocks. The details of the suggested system source and load parameters are tabulated in Table 1.

The suggested system and load parameters are offered in Table 1. Voltage sag compensation is carried out by the proposed control strategy based on these system parameters. Suppply voltage is applied across the load terminals without sag problems as soon as the powe source block is enerzised. The load voltage is

Table 1: The proposed system parameters for testing

	System parameters			Units	
Block	Name	Symbol	Value	Name	Symbol
3 phase source (ABC)	Line voltage	V_L	415	Volts	(V)
	Phase voltage	$V_{P = A,B,C}$	230	Volts	(V)
	Frequency	F	50	Hertz	(Hz)
Nonlinear load	Resistance	R	31.840	Ohm	(Ω)
	Inductance	L	0.139	Henry	(H)

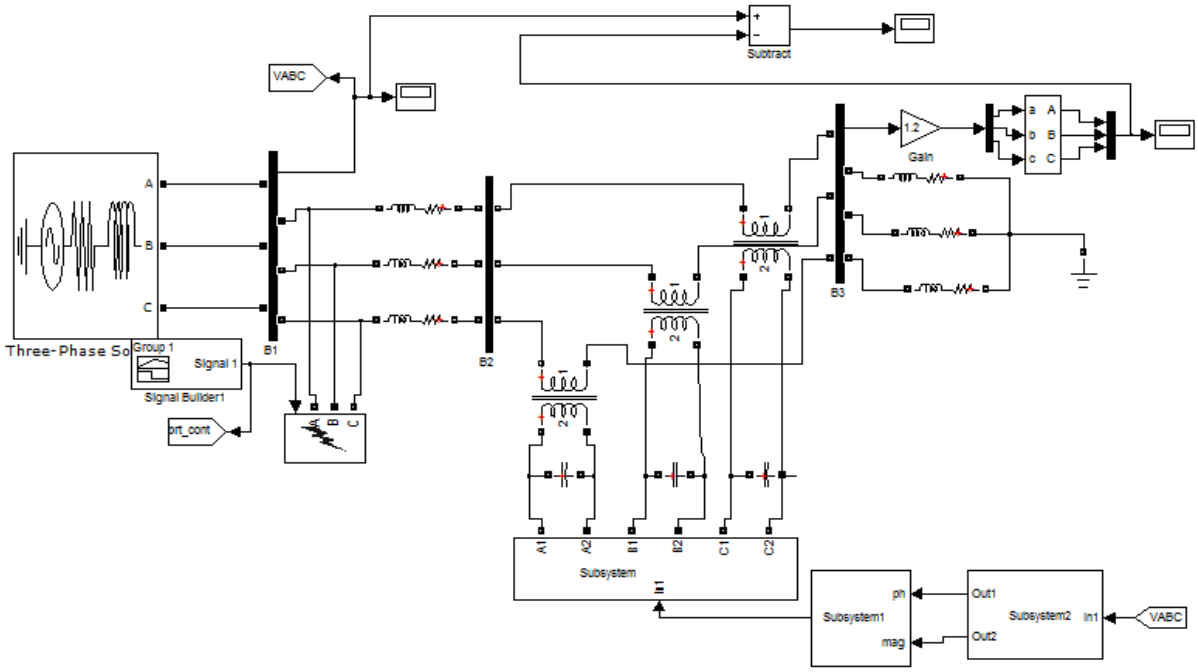

Fig. 6: The SIMULINK model of proposed system

Table 2: The testing conditions for proposed system

	Sag time (in sec)	
Fault timing	Start time	Stop time
Begin	0.0000	0.0700
Middle	0.1000	0.1640
End	0.1750	0.2495

clean sinusoidal and no alteration appears in this scenario. Once, the fault is brought into the system at line L1, which is the line joining buses B1 and B2. The voltage sag emerges across the load bus B3 due to the fault occurrence in line L1. DVR should be stimulated and employed for compensation in order to safeguard the load voltage and protect the nonlinear load. DVR is joined at line L2 which is the line joining buses B2 and B3. The performance of the proposed system is tested at different fault timings. In Table 2, the details of voltage sag occurrence timings in the system are tabulated.

Three different fault timings are given in Table 2. During these timings, voltage sag is brought into the system and verified for proposed method compensation. The intention of the suggested method over prior controllers of DVR is that, it has a precise estimation model based on EKF which identifies the sag appearance ahead and offers the suitable compensation to guard the sensitive load. In this issue, its superiority is confirmed by comparing with LKF aided controller and conventional DVR controller. The comparison is executed based on the presentation of injected voltage. Initially, the presentation of conventional DVR controller based supply voltage, load voltage and injected voltage is examined. In the subsequent graphs, the scale is specified as; simulation time in "seconds" is symbolized by X-axis where as Y-axis symbolizes the related parameter from the above. They are given as follows.

In Fig. 7, during commencing time of the simulation the supply voltage with sag and related load voltage due to the conventional controller is offered. The total simulation time for this test condition and its subsequent tests is 0.2500 sec. From Fig. 7, it states, the supply voltage has around 80 V dip in it due to the fault occurrence at bus B1 as the actual employed supply voltage is 230 V. By conventional controller this sag affected supply voltage is compensated. The load voltage is given after the compensation by the conventional controller. However, it is not up to the

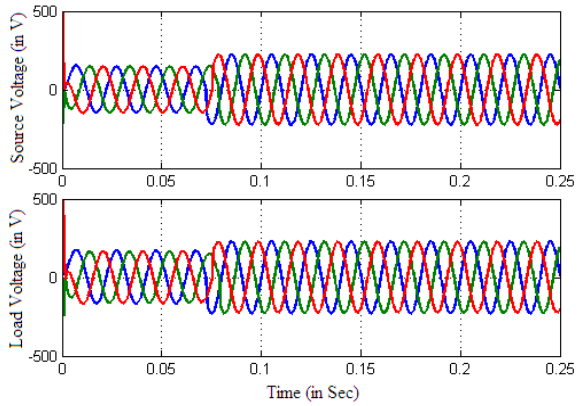

Fig. 7: Source and load voltage performance of conventional controller during fault at begin

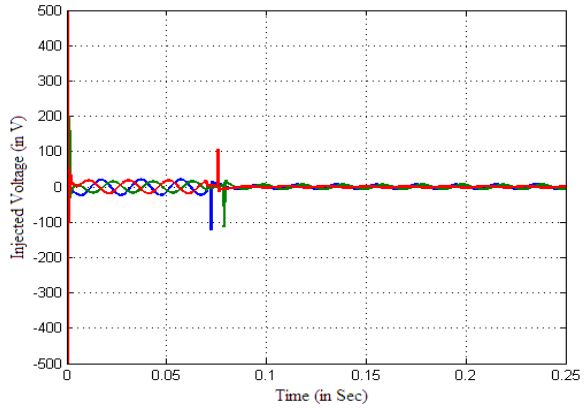

Fig. 8: Injected voltage performance of conventional controller during fault at begin

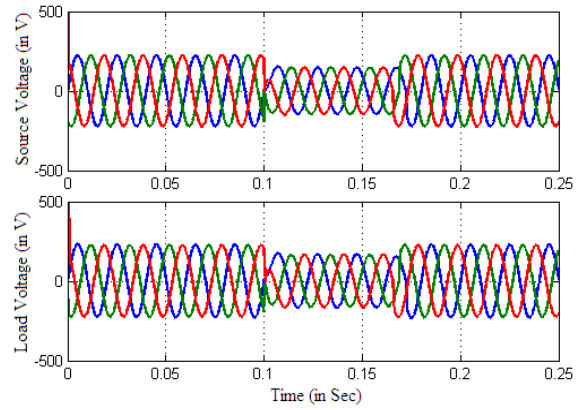

Fig. 9: Source and load voltage performance of conventional controller during fault at middle

mark of actual supply voltage, 230 V. In Fig. 8, the injected voltage by the conventional controller is offered. With this injected voltage from Fig. 8, it states that, the load voltage did not reach the needed value for sensitive load. Likewise, with similar voltage dip of 80 V, the conventional controller is verified during middle and end time of the simulation.

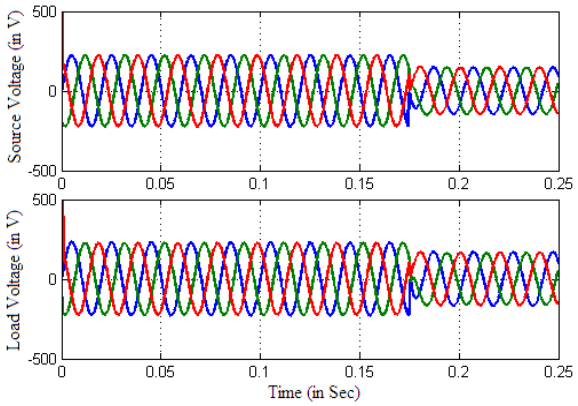

Fig. 10: Source and load voltage performance of conventional controller during fault at end

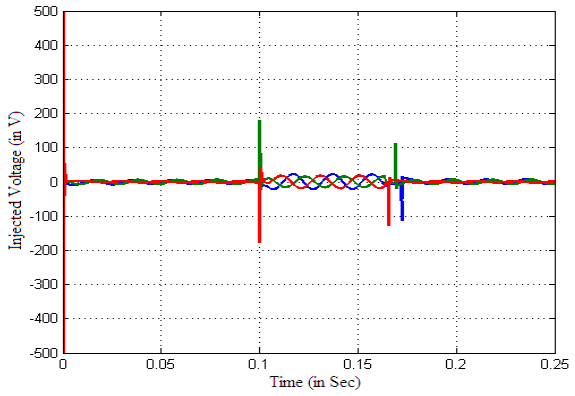

Fig. 11: Injected voltage performance of conventional controller during fault at middle

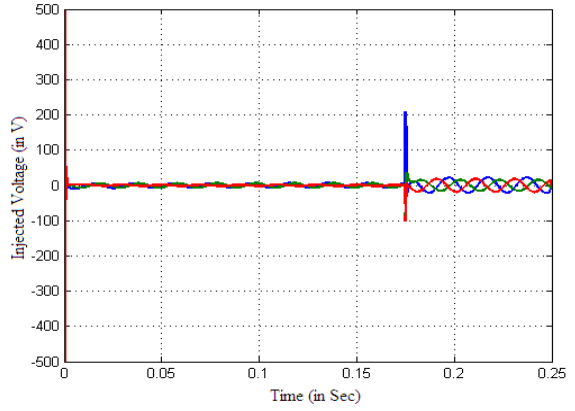

Fig. 12: Injected voltage performance of conventional controller during fault at end

The supply voltage and load voltage performance are offered in Fig. 9 and 10 due to the conventional controller of DVR during middle and end times of the simulation, respectively. In these scenarios also, the conventional controller could not accomplish the desired load voltage. The respected injected voltages by conventional controller are offered in Fig. 11 and 12.

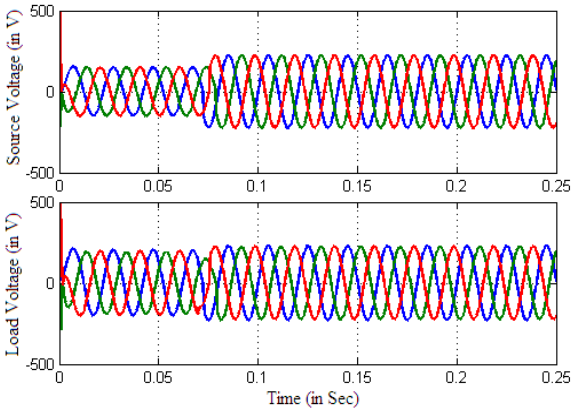

Fig. 13: Source and load voltage performance of LKF aided controller during fault at begin

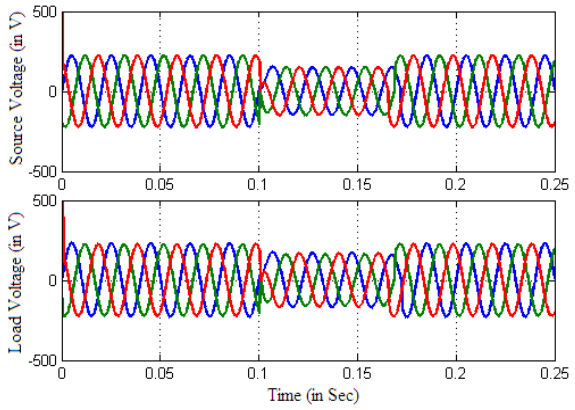

Fig. 14: Source and load voltage performance of LKF aided controller during fault at middle

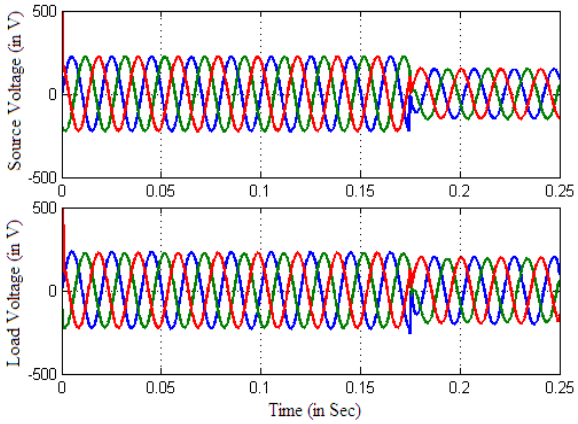

Fig. 15: Source and load voltage performance of LKF aided controller during fault at end

Now, the performance of LKF aided controller of DVR is examined. In this controller, LKF is employed to calculate approximately the symmetrical components of the calculated supply voltages. Control module is proposed for sag compensation based on the estimated

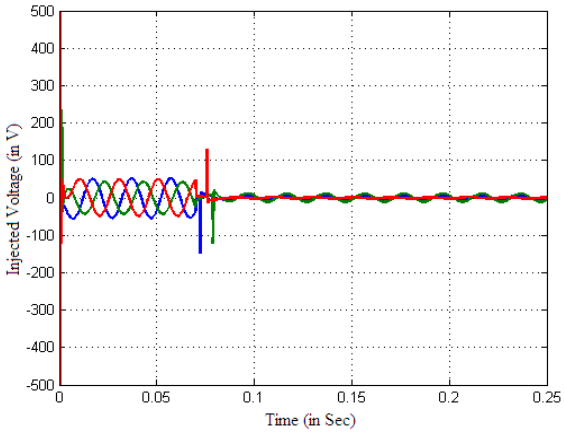

Fig. 16: Injected voltage performance of LKF aided controller during fault at begin

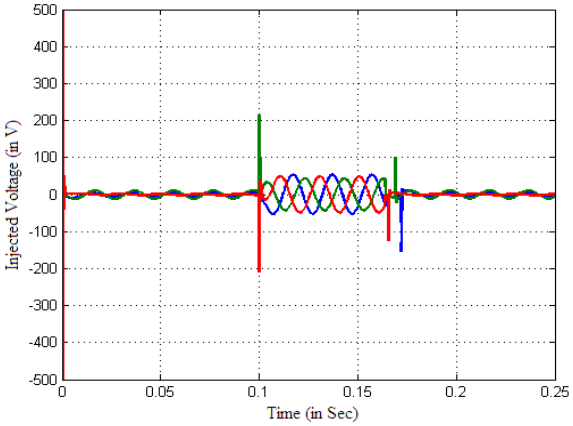

Fig. 17: Injected voltage performance of LKF aided controller during fault at middle

symmetrical components. LKF basis controller is as well examined for three different timings to verify its performance; begin middle and end timing of the simulation. The subsequent graphs are the performances of supply, load and injected voltages with the similar scale as in conventional.

In Fig. 13 to 15, the presentation of supply and load voltages of DVR system due to the LKF basis controller are offered. Owing to this controller, the load voltages are enhanced from conventional controller in three conditions and are close to the desired voltage with a dip of 30 V which is better than 80 V. The relevant injected voltages by LKF basis controller are offered in Fig. 16 to 18. These graphs demonstrate a slight enhancement from conventional controller however not sufficient for any kind of sensitive load.

Now, the performance of the proposed controller based on EKF is examined. It is as well tested under the same conditions with similar scale as before. The supply, load and injected voltages performance are specified as follows.

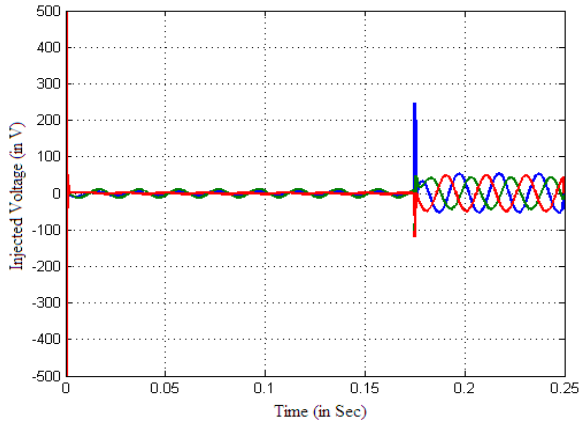

Fig. 18: Injected voltage performance of LKF aided controller during fault at end

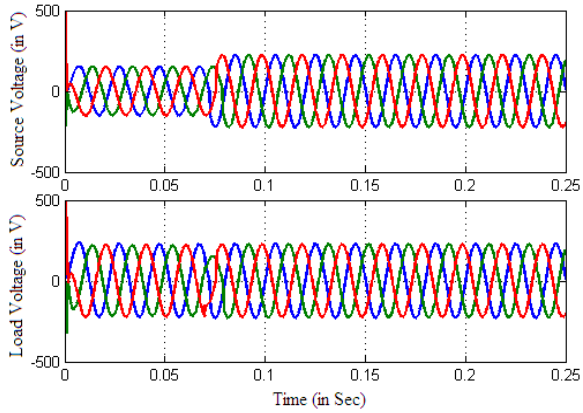

Fig. 19: Source and load voltage performance of proposed controller during fault at begin

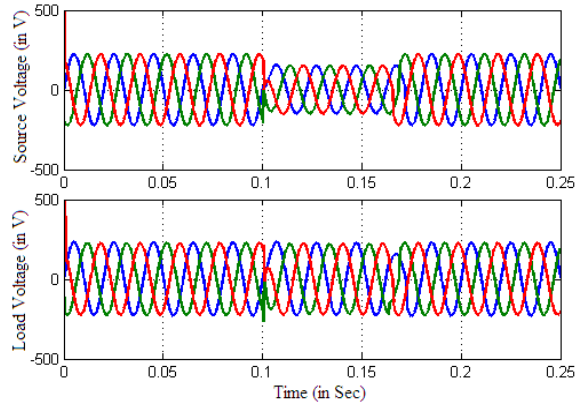

Fig. 20: Source and load voltage performance of proposed controller during fault at middle

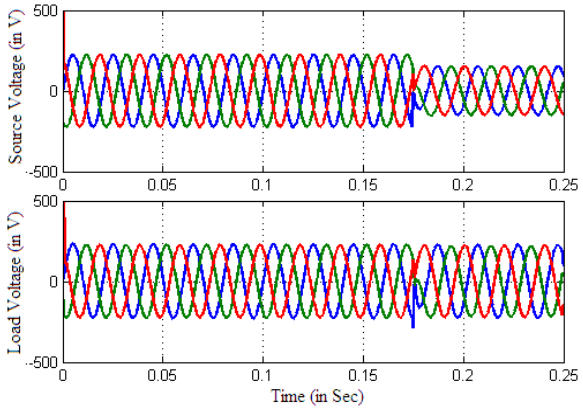

Fig. 21: The source voltage and load voltage during sag at end time of the simulation

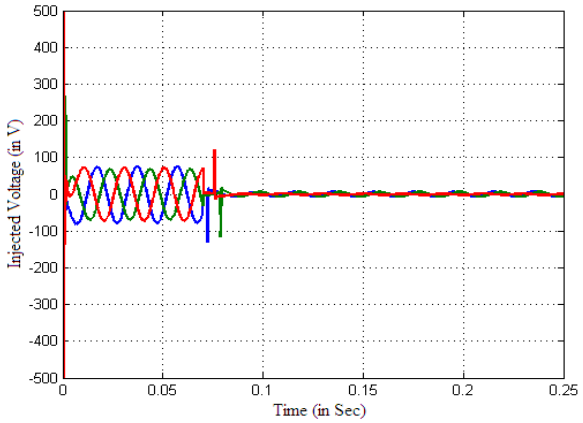

Fig. 22: Injected voltage performance of proposed controller during fault at begin

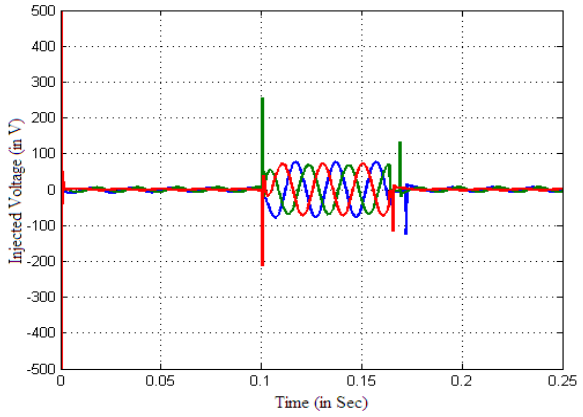

Fig. 23: Injected voltage performance of proposed controller during fault at middle

The performance of supply and load voltages due to the proposed controller is offered in Fig. 19 to 21. With the proposed controller, load voltages are enhanced from conventional controller and LKF basis controller in 3 fault conditions and are the same to the needed voltage, 230 V without a dip. The load voltage by proposed controller for all test conditions has essential sinusoidal voltages. For all test conditions there is small alteration in load voltage at start and last of compensation period. This is not essential to be

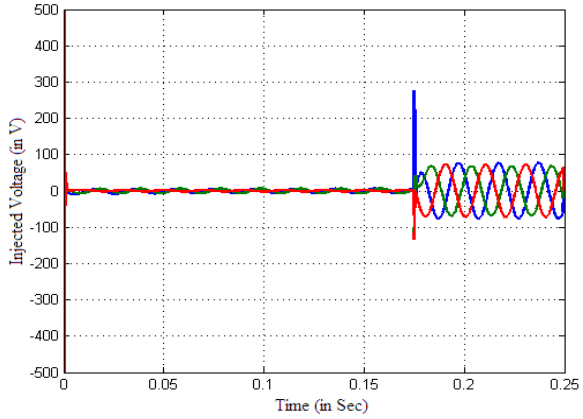

Fig. 24: Injected voltage performance of proposed controller during fault at end

alarmed as it is unimportant. In Fig. 22 to 24 the respective injected voltages by proposed controller are offered. This is the desired voltage better than conventional controller and LKF basis controller for any sensitive load. Now, the performances of conventional, LKF basis controller and proposed controller are evaluated by tabulating performance values in Table 3.

From the Table 3, it states that, for three controllers, source voltage due to the fault occurrence is 150 V. It is similar for all fault timings. For this sag of 80 V, the conventional controller has inserted 20, 22 and 20 V and reimbursed the load voltage to 170, 172 and 170 V correspondingly for 3 fault timings. Likewise, LKF basis controller has injected 50 V and reimbursed load voltage 200 V for 3 fault timings. In the same way, proposed controller has inserted 80, 78 and 80 V and reimbursed the load voltage to 230, 228 and 230 V for 3 fault timings correspondingly. Load voltage reimbursed up to 230 V is the acceptable one for any sensitive load. This compensation performance has confirmed the superiority of the proposed controller over conventional and LKF based controllers. The superior performance of proposed controller and LKF basis controller than conventional one is calculated by subsequent computation:

$$IP_{controller} = \frac{V_{L,controller} - V_{L,conventional}}{V_{L,conventional}} \times 100\% \quad (19)$$

where, $IP_{controller}$ is the enhanced performance of the controller. $V_{L,controller}$ and $V_{L,controller}$ are the load voltage performance value of stated controller and conventional controller respectively. The enhanced performance of the proposed and LKF basis controller are calculated by means of Eq. (19) and is tabulated in Table 4.

From Table 4, it explains that, during begin and end time of the simulation, proposed controller has 17.64% enhancement and during middle time of the simulation, it has 17.44% enhancement than the LKF basis controller. As a result, the proposed controller has better enhanced performance than LKF basis controller. Now, the performance comparison of three techniques is examined in terms of positive sequence components estimation.

In Fig. 25 to 27, the presentation of positive sequence amplitudes due to conventional, LKF basis controller and proposed controller are compared for three dissimilar fault timings. The scale of the above graphs is; simulation time in "seconds" on X-axis and positive sequence amplitude in "p.u." on Y-axis. The simulation time is up to 0.2500 sec only as this estimation comparison is executed for mentioned controllers during mentioned fault timings. From the assessments, it states that, proposed controller has excellent estimation than LKF basis controller and

Table 3: The performance comparison of the mentioned controllers

			Conventional controller	
Fault time	Source voltage during fault (in V)	Sag amplitude due to fault (in V)	Load voltage (in V)	Injected voltage (in V)
Begin	150	80	170	20
Middle	150	80	172	22
End	150	80	170	20
	LKF aided controller		Proposed controller	
Fault time	Load voltage (in V)	Injected voltage (in V)	Load voltage (in V)	Injected voltage (in V)
Begin	200	50	230	80
Middle	200	50	228	78
End	200	50	230	80

Table 4: The improved performance of proposed and LKF basis controller

	Improved performance of controllers than conventional one (in %)	
Fault time	LKF basis controller	Proposed controller
Begin	17.65	35.29
Middle	16.28	33.72
End	17.65	35.29

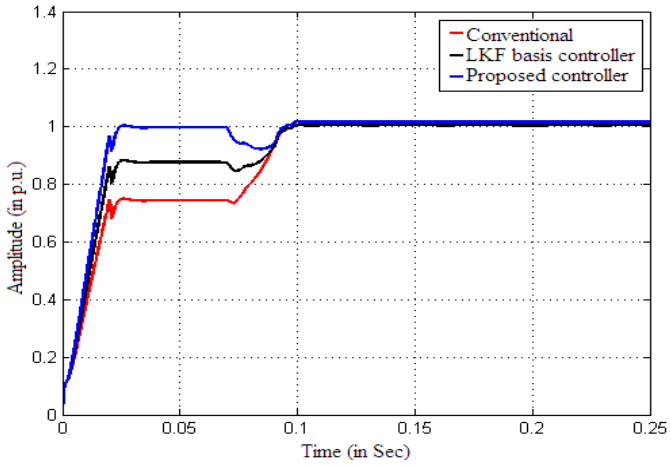

Fig. 25: Comparison performance of positive sequence amplitude for all controllers during fault at begin

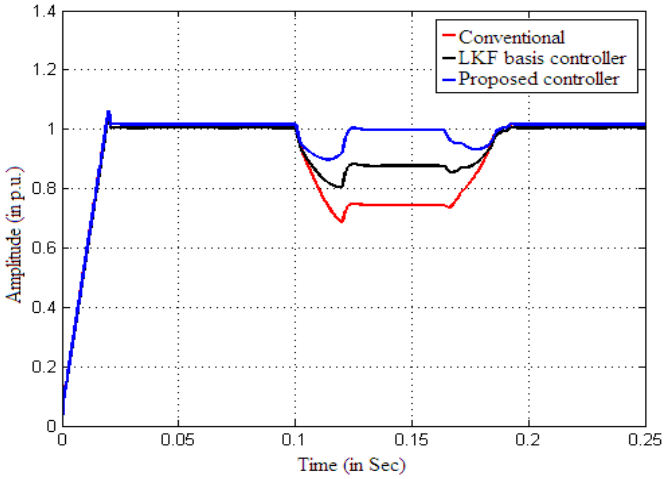

Fig. 26: Comparison performance of positive sequence amplitude for all controllers during fault at middle

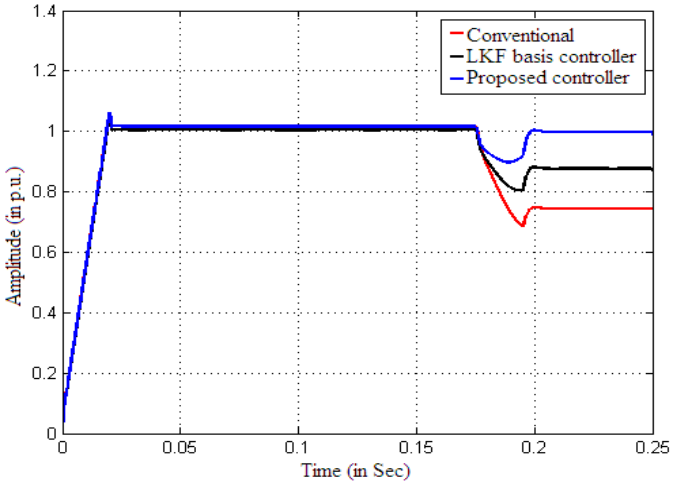

Fig. 27: Comparison performance of positive sequence amplitude for all controllers during fault at end

conventional controller. In Table 5 the comparison of performance values of the mentioned methods are tabulated.

From Table 5, it states that, proposed controller has estimated positive sequence amplitude up to 0.9 p.u. which is superior to the conventional and LKF one.

Table 5: Comparison performance of positive sequence amplitude estimation

	Positive sequence component amplitude (in p.u.) during fault		
Control technique	Begin	Middle	End
Conventional	0.70	0.70	0.70
LKF basis	0.80	0.80	0.80
Proposed	0.90	0.90	0.90

From this estimation comparisons and injection voltage comparisons, it is done that the proposed controller based on EKF model has better performance than conventional and LKF basis controller for sag compensation.

CONCLUSION

A novel estimation model for sag compensation by DVR is offered in this document. Based on EKF model the estimation model is presented. The suggested EKF based estimation model is employed to help the control algorithm for generating reference signals of PWM. As a result, DVR offers the compensation voltage as its output which is inserted in the connected line. This action nullifies the sag appearance. Voltage sag issues are identified precisely and fast performance is attained with the suggested estimation technique. This type of performance is answerable for guarding the sensitivity load. The presentation of the suggested estimation technique is examined in terms of providing the fundamental sinusoidal waveform to the nonlinear sensitive load. The validation of the suggested estimation algorithm was executed on MATLAB working platform. For conventional, LKF basis and proposed controllers simulation effects are inspected. From the comparison results, it is explained that the proposed controller has improved performance in compensating load voltage and estimating symmetrical components.

REFERENCES

Abdollahzadeh, H., M. Jazaeri and A. Tavighi, 2014. A new fast-converged estimation approach for Dynamic Voltage Restorer (DVR) to compensate voltage sags in waveform distortion conditions. Int. J. Elec. Power, 54: 598-609.

Ajaei, F.B., S. Afsharnia, A. Kahrobaeian and S. Farhangi, 2011. A fast and effective control scheme for the dynamic voltage restorer. IEEE T. Power Deliver., 26(4): 2398-2406.

Ajaei, F., S. Farhangi and R. Iravani, 2013. Fault current interruption by the dynamic voltage restorer. IEEE T. Power Deliver., 28(2): 903-910.

Babaei, E., M. Kangarlu and M. Sabahi, 2010. Mitigation of voltage disturbances using dynamic voltage restorer based on direct converters. IEEE T. Power Deliver., 25(4): 2676-2683.

Deepa, S. and S. Rajapandian, 2010. Voltage sag mitigation using dynamic voltage restorer system. Int. J. Comput. Electr. Eng., 2(5): 821-825.

Dib, S., B. Ferdi and C. Benachaiba, 2011. Adaptive neuro-fuzzy inference system based DVR controller design. Leonardo Electron. J. Pract. Technol., 18: 49-64.

El-Gammal, M.A., A.Y. Abou-Ghazala and T.I. El-Shennawy, 2011. Dynamic Voltage Restorer (DVR) for voltage sag mitigation. Int. J. Electr. Eng. Inform., 3(1): 1-11.Ghosh, H., P.K. Shah and G.K. Panda, 2012. Design and simulation of a novel self supported Dynamic Voltage Restorer (DVR) for power quality improvement. Int. J. Sci. Eng. Res., 3(6): 5.

Gupta, S.K., H.P. Tiwari and R. Pachar, 2010. Estimation of DC voltage storage requirements for dynamic voltage compensation on distribution network using DVR. IACSIT Int. J. Eng. Technol., 2(1): 124-131.

Hannan, M. and A. Mohamed, 2012. Study of basic properties of an enhanced controller for DVR compensation capabilities. Prz. Elektrotechniczn., 88(4a): 293-299.

Hussain, R. and J. Praveen, 2012. Voltage sag mitigation using distribution static compensator system. Int. J. Eng. Technol., 2(5): 756-760.

Ipinnimo, O., S. Chowdhury, S.P. Chowdhury and J. Mitra, 2013. A review of voltage dip mitigation techniques with distributed generation in electricity networks. Electr. Pow. Syst. Res., 103: 28-36.

Jayaprakash, P., B. Singh, D.P. Kothari, A. Chandra and K. Al-Haddad, 2014. Control of reduced-rating dynamic voltage restorer with a battery energy storage system. IEEE T. Ind. Appl., 50(2): 1295-1303.

Kandil, T., N.M. Ayad, A. Haleam and M. Mahmoud, 2013. Power quality problems mitigation using dynamic voltage restorer in Egypt thermal research reactor (ETRR- 2). Arab J. Nucl. Sci. Appl., 46(1): 347-358.

Kanjiya, P., B. Singh, A. Chandra and K. Al-Haddad, 2013. "SRF Theory Revisited" to control self-supported Dynamic Voltage Restorer (DVR) for unbalanced and nonlinear loads. IEEE T. Ind. Appl., 49(5): 2330-2340.

Kavitha, M., T. Chandrasekhar and D.M. Reddy, 2013. Designing of Dynamic Voltage Restorer (DVR) to improve the power quality for restructured power systems. Am. J. Electr. Power Energ. Syst., 2(3): 94-97.

Marefatjou, H. and M. Sarvi, 2012. Compensation of single-phase and three-phase voltage sag and swell using dynamic voltage restorer. Int. J. Appl. Power Eng., 1(3): 129-144.

Pakharia, A. and M. Gupta, 2012. Dynamic voltage restorer for compensation of voltage sag and swell: A literature review. Int. J. Adv. Eng. Technol., 4(1): 347-355.

Raman, J. and A. Singh, 2014. Mitigation of voltage sags by dynamic voltage restorer. J. Automat. Control Eng., 2(1): 49-53.

Singh, H., P. Arora and B. Singh, 2013. Voltage SAG mitigation by fuzzy controlled DVR. Int. J. Adv. Electr. Electron. Eng., 2(6): 93-100.

Tanti, D.K., M.K. Verma, B. Singh and O.N. Mehrotra, 2012. Optimal placement of custom power devices in power system network to mitigate voltage sag under faults. Int. J. Power Electron. Drive Syst., 2(3): 267-276.

Tiwari, H.P. and S.K. Gupta, 2010a. DC energy storage schemes for DVR voltage sag mitigation system. Int. J. Comput. Theor. Eng., 2(3): 313-318.

Tiwari, H.P. and S.K. Gupta, 2010b. Dynamic voltage restorer against voltage sag. Int. J. Innov. Manage. Technol., 1(3): 232-237.

Torres, A.P., P. Roncero-Sanchez, X. del Toro Garcia and V. Feliu, 2013. Design and comparison of two control strategies for voltage-sag compensation using dynamic voltage restorers. Elektron. Elektrotech., 19(6): 7-12.

Vetrivel, A., J. Jerome and N. Malmurugan, 2013. A novel method of voltage sag and swell estimation for power system applications. Am. J. Eng. Appl. Sci., 6(2): 233-240.